Springer

KSME

Journal of Mechanical Science and Technology 24 (12) (2010) 2529~2537
www.springerlink.com/content/1738-494x
DOI 10.1007/s12206-010-0917-z

Volume integral equation method for multiple isotropic inclusion problems in an infinite solid under tension or in-plane shear †

Jungki Lee*

Department of Mechanical and Design Engineering, Hongik University, Jochiwon-Eup, Yeonki-Gun, Chungnam, 339-701, Korea

(Manuscript Received January 29, 2010; Revised August 30, 2010; Accepted October 11, 2010)

Abstract

A volume integral equation method (VIEM) is introduced for the solution of elastostatic problems in an unbounded isotropic elastic solid containing interacting multiple isotropic inclusions subject to uniform remote tension or in-plane shear. This method is applied to two-dimensional problems involving long parallel cylindrical inclusions. A detailed analysis of the stress field at the interface between the matrix, and the central inclusion is carried out for square and hexagonal packing of the inclusions. The effects of the number of isotropic inclusions and various fiber volume fractions on the stress field at the interface between the matrix and the central inclusion are also investigated in detail. The accuracy and efficiency of the method are examined in comparison with results obtained from analytical and finite element methods.

Keywords: Volume integral equation method; Composite materials; Multiple inclusions; Fiber volume fraction; Finite element method

1. Introduction

Stress analysis of heterogeneous solids generally requires the use of numerical approaches based on the finite element or boundary element formulations. Both methods present difficulties in dealing with problems involving infinite media or multiple inclusions. It has been demonstrated that the volume integral formulation can overcome both of these limitations in heterogeneous problems involving infinite media [1, 2].

In contrast to the boundary integral equation method (BIEM), since the continuity condition at each interface is automatically satisfied in the volume integral equation formulation, it is not necessary to apply continuity conditions at each interface. Also, the method is not sensitive to the geometry of the inclusions. Moreover, in contrast to FEM, where the full domain needs to be discretized, the VIEM requires discretization of the multiple inclusions only.

The problem of a single inclusion or multiple inclusions in an infinite elastic solid under uniaxial tension has been examined by several authors (e.g., Eshelby [3], Hashin [4], Achenbach and Zhu [5], Christensen [6], Nimmer et al. [7], Zahl and Schmauder [8], Lee and Mal [9], Naboulsi [10], Aghdam and Falahatgar [11], Lee et al. [12], Ju and Ko [13] and Lee [14]). The problem of a single void or inclusion or multiple inclusions in an infinite elastic solid under in-plane shear has also been investigated by several authors (e.g., Jeffery [15], Ghosh and Ramberg [16], Cherkaev et al. [17], Shen et al. [18], Schmid [19], Schmid and Podladchikov [20], Treagus and Lan [21], Shimomura and Hasegawa [22], Vigdergauz [23] and Wang et al. [24]).

This paper is concerned with the analysis of the stress field in a heterogeneous elastic solid containing square and hexagonal packing of elastic isotropic circular inclusions embedded in an unbounded isotropic elastic matrix subject to remote uniaxial tension or in-plane shear using the volume integral equation method. The inclusions and the matrix are assumed to be isotropic. Of particular interest here is the influence of the geometry and number of inclusions and various fiber volume fractions on the stress field at the interface between the matrix and the central inclusion for square and hexagonal packing of the inclusions where the fiber volume fraction varies from 0.20 to 0.50 in increments of 0.05. It is demonstrated that the volume integral equation method is very accurate and effective for investigating the local stresses in composites containing multiple fibers.

2. Volume integral equation method

The geometry of the general elastostatic problem considered here is shown in Fig. 1 where an unbounded isotropic elastic solid containing inclusions of arbitrary shape is subjected to

† This paper was recommended for publication in revised form by Associate Editor Chang-Wan Kim

* Corresponding author. Tel.: +82 41 860 2619, Fax.: +82 41 866 9129
E-mail address: inq3jkl@wow.hongik.ac.kr

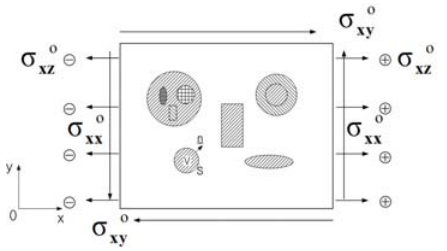

Fig. 1. Geometry of the general elastostatic problem.

prescribed loading at infinity. Let $c_{ijkl}^{(1)}$ denote the elastic stiffness tensor of the inclusion and $c_{ijkl}^{(2)}$ those of the isotropic matrix material. The matrix is assumed to be homogeneous and isotropic so that $c_{ijkl}^{(2)}$ is a constant isotropic tensor, while $c_{ijkl}^{(1)}$ is arbitrary, i.e., the inclusions may, in general, be inhomogeneous and anisotropic. The interfaces between the inclusions and the matrix are assumed to be perfectly bonded ensuring continuity of the displacement and stress vectors.

Mal and Knopoff [25] and Lee and Mal [1] have shown that the elastostatic displacement in the composite satisfies the volume integral equation,

$$u_m(\mathbf{x}) = u_m^o(\mathbf{x}) - \int_R \delta c_{ijkl} g_{i,j}^m(\xi, \mathbf{x}) u_{k,l}(\xi) d\xi, \qquad (1)$$

where the integral is over the whole space, $\delta c_{ijkl} = c_{ijkl}^{(1)} - c_{ijkl}^{(2)}$, and $g_i^m(\xi, \mathbf{x})$ is the static Green's function (or Kelvin's solution) for the unbounded matrix material, i.e., $g_i^m(\xi, \mathbf{x})$ represents the *i*th component of the displacement at ξ due to unit concentrated force at $\mathbf{x}$ in the *m*th direction. In Eq. (1), the summation convention and comma notation have been used and the differentiations are with respect to ξ_i. The integrand is non-zero within the inclusions only, since $\delta c_{ijkl} = 0$, outside the inclusions.

If $\mathbf{x} \in R$, then Eq. (1) is an integrodifferential equation for the unknown displacement vector $\mathbf{u}(\mathbf{x})$, and it can, in principle, be determined through the solution of Eq. (1). An algorithm based on the discretization of Eq. (1) was developed in Lee and Mal [1, 2] to determine $\mathbf{u}(\mathbf{x})$ by discretizing the inclusions using standard finite elements. Once $\mathbf{u}(\mathbf{x})$ within the inclusions is determined, the displacement field in the matrix can be obtained from Eq. (1) by evaluating the integral. The stress field within and outside the inclusions can also be determined in a similar manner. Details of the numerical treatment of Eq. (1) for plane elastodynamic and elastostatic problems can be found in [1, 2]. A detailed explanation for the volume integral equation method involving multiple isotropic inclusions in the unbounded isotropic matrix can also be found in Section 4.3 "Volume Integral Equation Method" by Buryachenko [26].

3. Multiple inclusion problems

We consider plane strain problems for multiple isotropic cylindrical inclusions in the unbounded isotropic matrix under uniform remote tensile loading, σ_{xx}^o, as shown in Fig. 2 and under remote in-plane shear, σ_{xy}^o, as shown in Fig. 3.

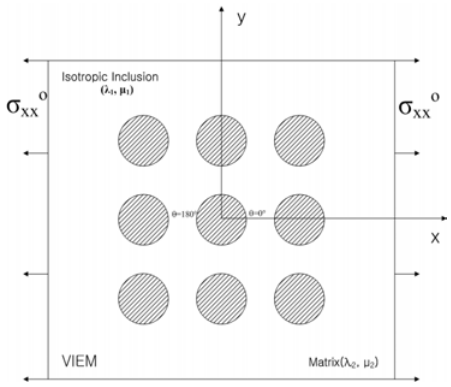

Fig. 2. Multiple isotropic cylindrical inclusions in the unbounded isotropic matrix under uniform remote tensile loading.

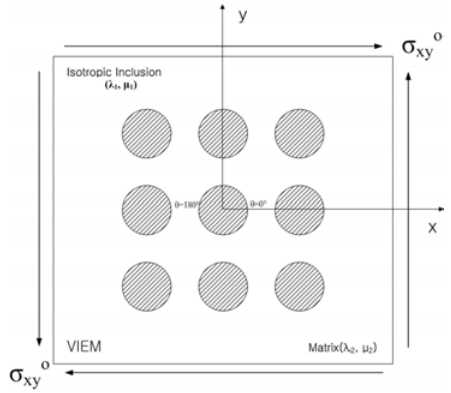

Fig. 3. Multiple isotropic cylindrical inclusions in the unbounded isotropic matrix under remote in-plane shear loading.

A detailed analysis of the stress field at the interface between the matrix and the central isotropic inclusion is carried out for square and hexagonal packing containing different numbers of inclusions in the unbounded matrix where the fiber volume fraction is 0.20, 0.25, 0.30, 0.35, 0.40, 0.45, and 0.50.

For this problem, it is most advantageous to apply the volume integral equation method [1, 26]. This is due to the fact that, in contrast to the boundary integral equation method (BIEM), since the continuity condition at each interface is automatically satisfied in the volume integral equation formulation, it is not necessary to apply continuity conditions at each interface. Also, the method is not sensitive to the geometry, anisotropy, and inhomogeneity of the inclusions. Moreover, in contrast to FEM, where the full domain needs to be discretized, the VIEM requires discretization of the multiple inclusions only. Specifically, when the fiber volume fraction varies from 0.20 to 0.50 in increments of 0.05, the position of the inclusions only needs to be changed in the VIEM model.

3.1 Green's function for the unbounded isotropic material

In Eq. (1), $g_i^m(\xi, \mathbf{x})$ is Green's function for the unbounded isotropic matrix material and is given by Banerjee [27]

Table 1. Material properties of the isotropic matrix and the isotropic inclusion for the elastostatic problems.

(Unit: GPa)	Isotropic Matrix	Isotropic Inclusion
λ	67.34	176.06
μ	37.88	176.06

Table 2. Normalized tensile stress component ($\sigma_{xx}/\sigma_{xx}^{o}$) within the isotropic cylindrical inclusion due to uniform remote tensile loading (σ_{xx}^{o}).

	Normalized tensile stress component inside the isotropic inclusion
Exact	1.3167
VIEM	1.3167 (Average)

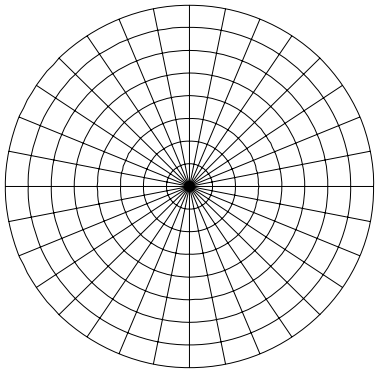

Fig. 4. A typical discretized model in the volume integral equation method.

$$g_{\alpha}^{\beta} = \frac{\lambda+\mu}{4\pi\mu(\lambda+2\mu)}[-\frac{\lambda+3\mu}{\lambda+2\mu}\ln r\delta_{\alpha\beta} + r_{,\alpha}r_{,\beta}], \quad (2)$$

where r = | **x** - **ξ** | and α, β = 1, 2 and λ, μ are the Lamé constants for the unbounded isotropic matrix material.

3.2 Multiple inclusion problems under uniform remote tensile loading

We first consider plane strain problems for multiple isotropic cylindrical inclusions in the unbounded isotropic matrix under remote tensile loading, σ_{xx}^{o}, as shown in Fig. 2.

3.2.1 Single inclusion problem

To check the accuracy of the volume integral equation method, we first consider a single isotropic cylindrical inclusion in the unbounded isotropic matrix under uniform remote tensile loading. The elastic constants for the isotropic matrix and the isotropic inclusion are listed in Table 1.

Fig. 4 shows a typical discretized model used in the VIEM [28]. A total of 256 standard eight-node quadrilateral and six-node triangular elements were used in the VIEM. The number of elements, 256, was determined based on a convergence test. Table 2 shows the comparison between the well-known analytical solution (see, e.g., Mal and Singh [29]) and the numerical solution using VIEM for the normalized tensile stress component ($\sigma_{xx}/\sigma_{xx}^{o}$) within the isotropic inclusion under uniform remote tensile loading (σ_{xx}^{o}). As expected, the tensile stress component inside the isotropic inclusion was found to be constant [1,29]. It can be seen that there is excellent agreement between the two sets of results.

Table 3. Fiber separation distances according to different fiber volume fractions.

Fiber volume fraction (c)	Fiber separation distance / Radius of inclusion (d/a)	
	Square array	Hexagonal array
0.20	3.9633	4.2589
0.25	3.5449	3.8093
0.30	3.2360	3.4774
0.35	2.9960	3.2194
0.40	2.8025	3.0115
0.45	2.6422	2.8392
0.50	2.5066	2.6935

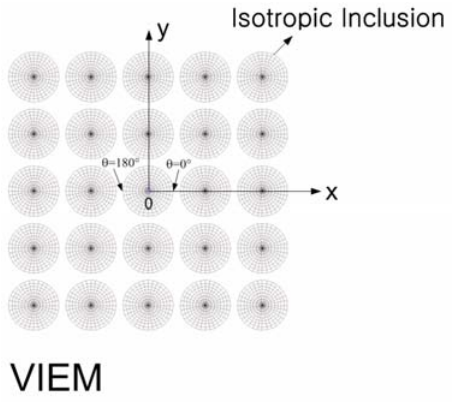

Fig. 5. A typical discretized model in the volume integral equation method.

3.2.2 Square packing of isotropic inclusions

Next, in order to analyze multiple-inclusion interactions, the square packing of (a) 9 inclusions, (b) 25 inclusions, and (c) 49 inclusions is considered where the fiber volume fraction is 0.20, 0.25, 0.30, 0.35, 0.40, 0.45 and 0.50. The elastic constants for the isotropic matrix and the isotropic inclusion are listed in Table 1. Table 3 shows fiber separation distances according to different fiber volume fractions. For example, the square packing sequence leads to a fiber separation distance d = 2.996a for c = 0.35, where 'a' represents the radius of each fiber.

Fig. 5 shows a typical discretized model used in the VIEM for a square packing sequence [28]. The standard eight-node quadrilateral and six-node triangular elements were used in the discretization. The number of elements used in each inclusion was 256 and was determined based on a convergence test.

Fig. 6 shows the normalized tensile stress component ($\sigma_{xx}/\sigma_{xx}^{o}$) at the interface between the matrix and the central inclusion for models containing a single inclusion and three different numbers (9, 25 and 49) of square arrays of inclusions where the fiber volume fraction (c) varies from 0.20 to 0.50 in increments of 0.05 (θ = 0°~360°). The interaction effect of a

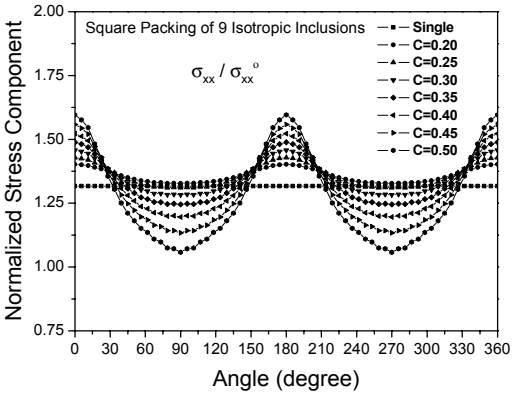

(a)

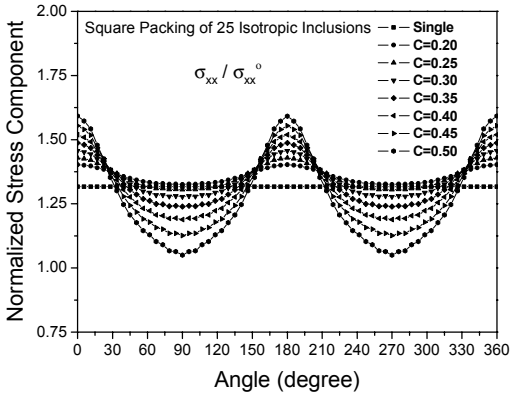

(b)

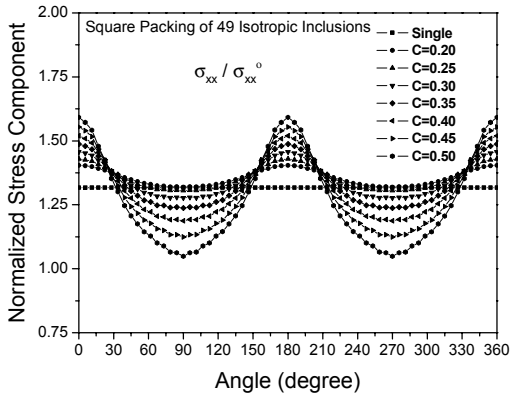

(c)

Fig. 6. Normalized tensile stress component ($\sigma_{xx}/\sigma_{xx}^{o}$) at the interface between the central isotropic inclusion and the isotropic matrix under uniform remote tensile loading for the square packing of inclusions.

square array of inclusions on the normalized tensile stress component ($\sigma_{xx}/\sigma_{xx}^{o}$) at the interface between the matrix and the central inclusion appears to be minimal for the same fiber volume fraction. However, as the fiber volume fraction increases, the normalized tensile stress component ($\sigma_{xx}/\sigma_{xx}^{o}$) at the interface between the matrix and the central inclusion differs noticeably for each case. This is because the interaction effect of a square array of inclusions on the normalized tensile stress component at the interface appears to become stronger as the fiber volume fraction increases.

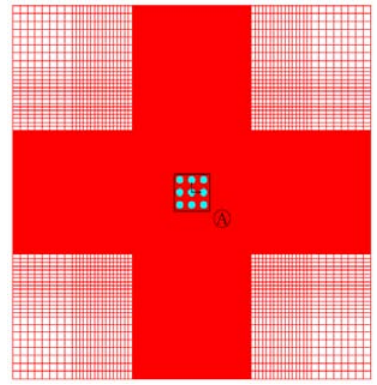

(a)

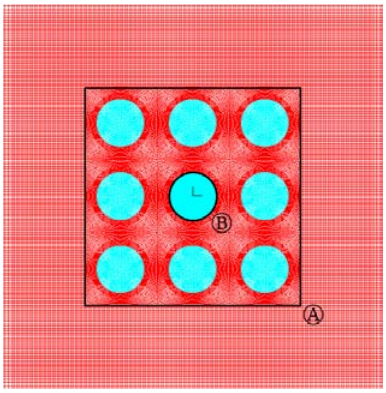

(b)

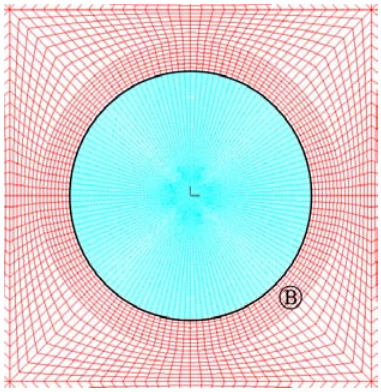

(c)

Fig. 7. A typical discretized model in the finite element method for a square inclusion packing array.

3.2.3 Verification of the VIEM solution

To check the accuracy of the volume integral equation method solution, the numerical solution using the volume integral equation method for square packing of nine inclusions with a volume concentration, c = 0.35, was compared with a numerical solution using the commercial finite element code ADINA [30].

Fig. 7 shows a typical finite element model using ADINA. Fig. 7(a) shows the total model, Fig. 7(b) shows an expanded view of the mesh surrounding the square packing of nine inclusions (represented as Ⓐ), and Fig. 7(c) shows an expanded view of the mesh surrounding the central inclusion (repre-

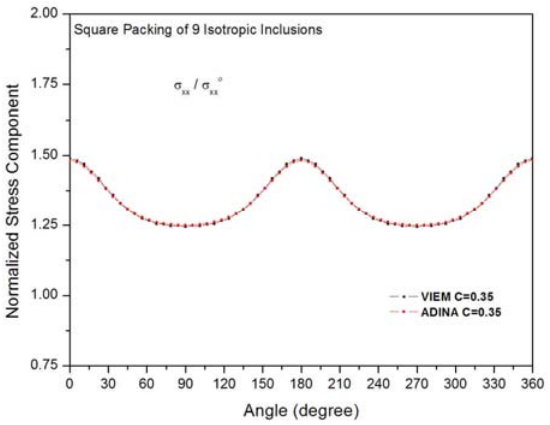

Fig. 8. Comparison of numerical solutions using the volume integral equation method and ADINA for the normalized tensile stress component ($\sigma_{xx}/\sigma_{xx}^{o}$) at the interface between the central isotropic inclusion and the isotropic matrix under uniform remote tensile loading for a square packing of inclusions.

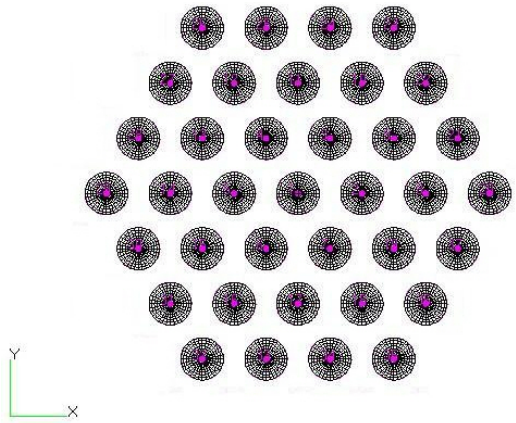

Fig. 9. A typical discretized model in the volume integral equation method for a hexagonal inclusion packing array.

sented as Ⓑ). The standard four-node quadrilateral and three-node triangular elements were used in the discretization. The total number of elements used in the model was 121,600. To capture the accurate stress distribution at the interface between the matrix and the central inclusion, very refined finite elements were used near the interfaces. The infinite dimensions of the matrix were approximated to be 22.5a in length, where 'a' represents the diameter of each inclusion. It can be easily seen that the discretized model in the volume integral equation method in Fig. 5 is much more effective than the discretized model in the finite element method in Fig. 7. In contrast to FEM, where the full domain needs to be discretized, the VIEM requires discretization of the multiple inclusions only. Specifically, when the fiber volume fraction varies from 0.20 to 0.50 in increments of 0.05, the position of the inclusions only needs to be changed in the VIEM model. Fig. 8 shows the comparison between the numerical solutions using VIEM and ADINA for the normalized tensile stress component ($\sigma_{xx}/\sigma_{xx}^{o}$) at the interface between the matrix and the central inclusion ($\theta = 0°\sim360°$). It can be seen that there is excellent agreement between the two sets of results [31].

3.2.4 Hexagonal packing of isotropic inclusions

Next, in order to analyze multiple-inclusion interactions, hexagonal packing of (a) 7 inclusions, (b) 19 inclusions, and (c) 37 inclusions is considered where the fiber volume fraction is 0.20, 0.25, 0.30, 0.35, 0.40, 0.45 and 0.50. The elastic constants for the isotropic matrix and the isotropic inclusion are listed in Table 1. Table 3 shows fiber separation distances according to different fiber volume fractions. For example, the hexagonal packing sequence leads to a fiber separation distance $d = 3.2194a$ for $c = 0.35$, where 'a' represents the radius of each fiber.

Fig. 9 shows a typical discretized model used in the VIEM for a hexagonal packing sequence [28]. The standard eight-node quadrilateral and six-node triangular elements were used in the discretization.

Fig. 10 shows the normalized tensile stress component ($\sigma_{xx}/\sigma_{xx}^{o}$) at the interface between the matrix and the central inclusion for models containing a single inclusion and three different numbers (7, 19 and 37) of hexagonal arrays of inclusions where the fiber volume fraction is 0.20, 0.25, 0.30, 0.35, 0.40, 0.45 and 0.50 ($\theta = 0°\sim360°$). The interaction effect of a hexagonal array of inclusions on the normalized tensile stress component ($\sigma_{xx}/\sigma_{xx}^{o}$) at the interface between the matrix and the central inclusion appears to be minimal for the same fiber volume fraction. However, as the fiber volume fraction increases, the normalized tensile stress component ($\sigma_{xx}/\sigma_{xx}^{o}$) at the interface between the matrix and the central inclusion differs noticeably for each case. This is because the interaction effect of a hexagonal array of inclusions on the normalized tensile stress component at the interface appears to become stronger as the fiber volume fraction increases.

Figs. 6 and 10 show that the normalized tensile stress component at the interface between the matrix and the central inclusion differs noticeably between square and hexagonal arrays of inclusions.

3.3 Multiple inclusion problems under remote in-plane shear

We next consider plane strain problems for multiple isotropic cylindrical inclusions in the unbounded isotropic matrix under remote in-plane shear, σ_{xy}^{o}, as shown in Fig. 3.

3.3.1 Single inclusion problem

To check the accuracy of the volume integral equation method, we first consider a single isotropic cylindrical inclusion in the unbounded isotropic matrix under remote in-plane shear. The elastic constants for the isotropic matrix and the isotropic inclusion are listed in Table 1.

Fig. 4 shows a typical discretized model used in the VIEM [28]. A total of 256 standard eight-node quadrilateral and six-node triangular elements were used in the VIEM.

Table 4 shows the comparison between the well-known

Table 4. Normalized shear stress component ($\sigma_{xy}/\sigma_{xy}^{o}$) within the isotropic cylindrical inclusion due to remote in-plane shear (σ_{xy}^{o}).

	Normalized shear stress component inside the isotropic inclusion
Exact	1.4056
VIEM	1.4056 (Average)

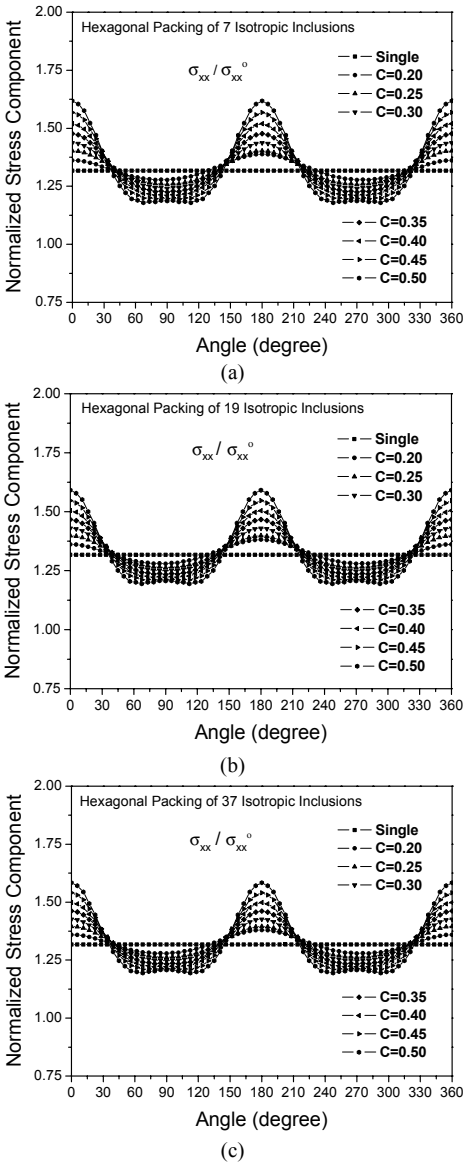

Fig. 10. Normalized tensile stress component ($\sigma_{xx}/\sigma_{xx}^{o}$) at the interface between the central isotropic inclusion and the isotropic matrix under uniform remote tensile loading for the hexagonal packing of inclusions.

analytical solution (see, e.g., Wang et al. [24]) and the numerical solution using VIEM for the normalized shear stress component ($\sigma_{xy}/\sigma_{xy}^{o}$) within the isotropic inclusion under remote in-plane shear (σ_{xy}^{o}). As expected, the shear stress component inside the isotropic inclusion was found to be constant [1,24]. It can be seen that there is excellent agreement between the two sets of results.

3.3.2 Square packing of isotropic inclusions

Next, in order to analyze multiple-inclusion interactions, square packing of (a) 9 inclusions, (b) 25 inclusions, and (c) 49 inclusions is considered where the fiber volume fraction is 0.20, 0.25, 0.30, 0.35, 0.40, 0.45 and 0.50. The elastic constants for the isotropic matrix and the isotropic inclusion are listed in Table 1. Table 3 shows fiber separation distances according to different fiber volume fractions. For example, the square packing sequence leads to a fiber separation distance d = 2.8025a for c = 0.40, where 'a' represents the radius of each fiber.

Fig. 5 shows a typical discretized model used in the VIEM for a square packing sequence [28].

Fig. 11 shows the normalized shear stress component ($\sigma_{xy}/\sigma_{xy}^{o}$) at the interface between the matrix and the central inclusion for models containing a single inclusion and three different numbers (9, 25 and 49) of square arrays of inclusions where the fiber volume fraction is 0.20, 0.25, 0.30, 0.35, 0.40, 0.45 and 0.50 ($\theta = 0°\sim360°$). The interaction effect of a square array of inclusions on the normalized shear stress component ($\sigma_{xy}/\sigma_{xy}^{o}$) at the interface between the matrix and the central inclusion appears to be minimal for the same fiber volume fraction. However, as the fiber volume fraction increases, the normalized shear stress component ($\sigma_{xy}/\sigma_{xy}^{o}$) at the interface between the matrix and the central inclusion differs noticeably for each case. This is because the interaction effect of a square array of inclusions on the normalized shear stress component at the interface appears to become stronger as the fiber volume fraction increases.

3.3.3 Hexagonal packing of isotropic inclusions

Next, in order to analyze multiple-inclusion interactions, hexagonal packing of (a) 7 inclusions, (b) 19 inclusions, and (c) 37 inclusions is considered where the fiber volume fraction is 0.20, 0.25, 0.30, 0.35, 0.40, 0.45 and 0.50. The elastic constants for the isotropic matrix and the isotropic inclusion are listed in Table 1. Table 3 shows fiber separation distances according to different fiber volume fractions. For example, the hexagonal packing sequence leads to a fiber separation distance d = 3.0115a for c = 0.40, where 'a' represents the radius of each fiber.

Fig. 9 shows a typical discretized model used in the VIEM for a hexagonal packing sequence [28].

Fig. 12 shows the normalized shear stress component ($\sigma_{xy}/\sigma_{xy}^{o}$) at the interface between the matrix and the central inclusion for models containing a single inclusion and three different numbers (7, 19 and 37) of hexagonal arrays of inclusions where the fiber volume fraction is 0.20, 0.25, 0.30, 0.35, 0.40, 0.45 and 0.50 ($\theta = 0°\sim360°$). The interaction effect of a hexagonal array of inclusions on the normalized shear stress component ($\sigma_{xy}/\sigma_{xy}^{o}$) at the interface between the matrix and the central inclusion appears to be minimal for the same fiber volume fraction. However, as the fiber volume fraction increases, the normalized shear stress component ($\sigma_{xy}/\sigma_{xy}^{o}$) at the interface between the matrix and the central inclusion differs

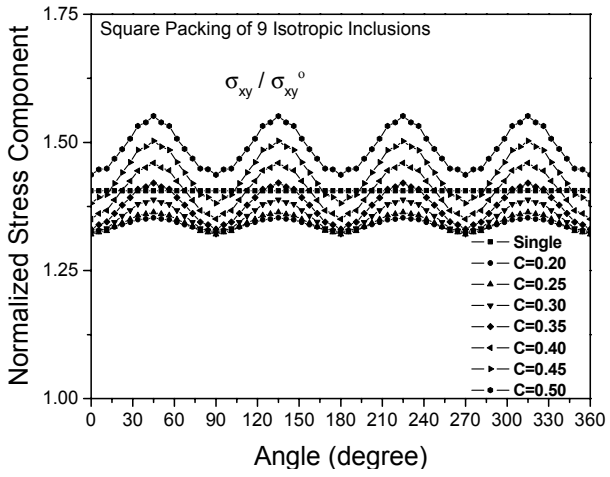

(a)

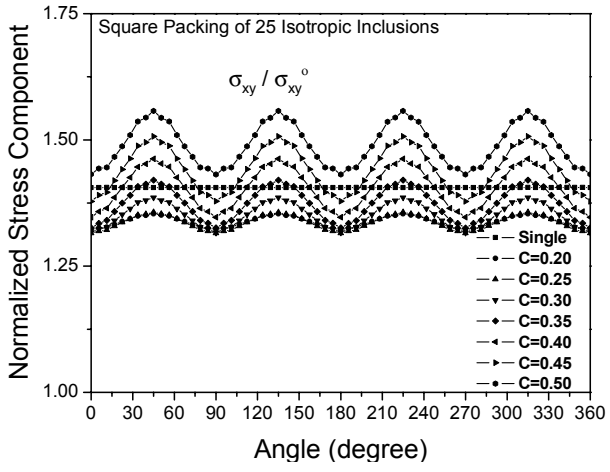

(b)

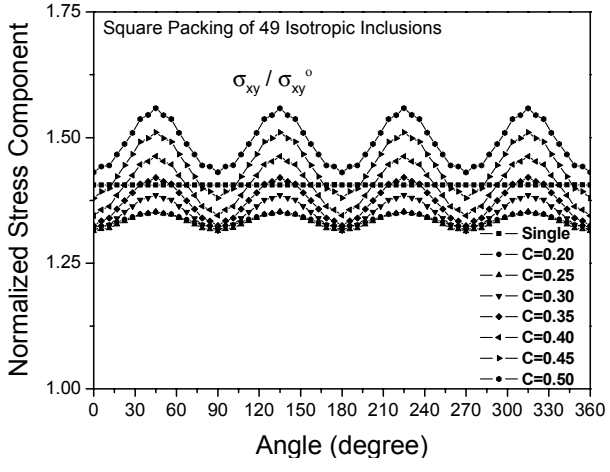

(c)

Fig. 11. Normalized shear stress component ($\sigma_{xy}/\sigma_{xy}^{o}$) at the interface between the central isotropic inclusion and the isotropic matrix under remote in-plane shear for the square packing of inclusions.

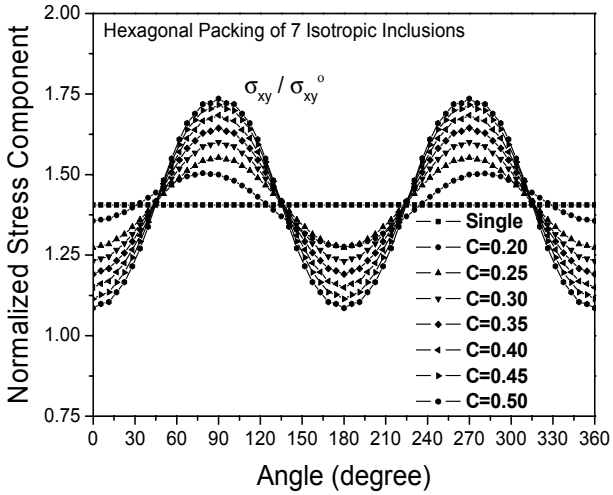

(a)

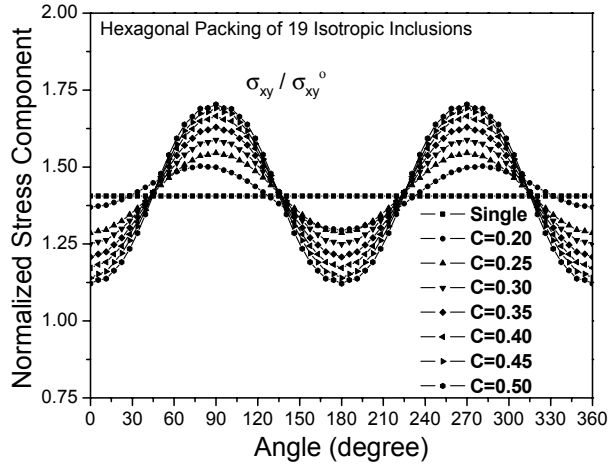

(b)

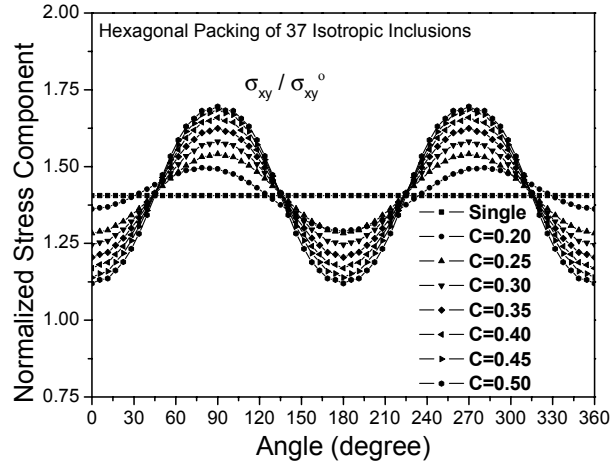

(c)

Fig. 12. Normalized shear stress component ($\sigma_{xy}/\sigma_{xy}^{o}$) at the interface between the central isotropic inclusion and the isotropic matrix under remote in-plane shear for the hexagonal packing of inclusions.

noticeably for each case. The reason is that the interaction effect of a hexagonal array of inclusions on the normalized shear stress component at the interface appears to become stronger as the fiber volume fraction increases.

Figs. 11 and 12 show that the normalized shear stress component at the interface between the matrix and the central inclusion differs significantly between square and hexagonal arrays of inclusions.

4. Conclusions

First, the interaction effect of square and hexagonal arrays of isotropic inclusions on the tensile stress component at the interface between the isotropic matrix and the central isotropic inclusion under uniform remote tensile loading was investigated where the fiber volume fraction was 0.20, 0.25, 0.30, 0.35, 0.40, 0.45 and 0.50. The interaction effect of square and hexagonal arrays of isotropic inclusions on the tensile stress component at the interface was minimal for the same fiber volume fraction. However, the interaction effect of square and hexagonal arrays of isotropic inclusions on the normalized tensile stress component at the interface became stronger as the fiber volume fraction increased.

Second, in order to check the accuracy of the volume integral equation method solution, the numerical solution using the volume integral equation method for square packing of nine inclusions with a volume concentration, c = 0.35, was compared to a numerical solution using the commercial finite element code ADINA [30]. There was excellent agreement between the two sets of results. Moreover, in contrast to FEM, where the full domain needs to be discretized, it was determined that the VIEM requires discretization of the multiple inclusions only. Particularly, when the fiber volume fraction varies from 0.20 to 0.50 in increments of 0.05, the position of the inclusions only needs to be changed in the VIEM model.

Third, the interaction effect of square and hexagonal arrays of isotropic inclusions on the shear stress component at the interface between the isotropic matrix and the central isotropic inclusion under remote in-plane shear was investigated where the fiber volume fraction was 0.20, 0.25, 0.30, 0.35, 0.40, 0.45 and 0.50. The interaction effect of square and hexagonal arrays of isotropic inclusions on the shear stress component at the interface was minimal for the same fiber volume fraction. However, the interaction effect of square and hexagonal arrays of isotropic inclusions on the normalized shear stress component at the interface became stronger as the fiber volume fraction increased.

Fourth, as expected, it was determined that the normalized tensile stress component at the interface between the matrix and the central inclusion for square and hexagonal arrays of inclusions differs significantly from the normalized shear stress component at the interface between the matrix and the central inclusion for square and hexagonal arrays of inclusions. Therefore, it is necessary to model the fibers under various types of loading conditions in order to accurately predict the failure and damage mechanisms in real composites.

Finally, through the analysis of plane elastostatic problems in an unbounded isotropic matrix with multiple isotropic inclusions, it was determined that the VIEM is very accurate and effective for investigating the stresses in composites containing arbitrary geometry and multiple isotropic inclusions.

Acknowledgment

This work was supported by the Small & Medium Business Administration (SMBA), 2009 Support Project for Establishment of Business Research Institute through Cooperation between Industry-Academia-Research Institute.

References

[1] J. K. Lee and A. K. Mal, A volume integral equation technique for multiple inclusion and crack interaction problems, *Transactions of the ASME*, *Journal of Applied Mechanics*, 64 (1997) 23-31.

[2] J. K. Lee and A. K. Mal, A volume integral equation technique for multiple scattering problems in elastodynamics, *Applied Mathematics and Computation*, 67 (1995) 135-159.

[3] J. D. Eshelby, The determination of the elastic field of an ellipsoidal inclusion, and related problems, *Proceedings of the Royal Society of London, Series A*, A241 (1957) 376-396.

[4] Z. Hashin, Theory of Fiber Reinforced Materials, NASA CR-1974 (1972).

[5] J. D. Achenbach and H. Zhu, Effect of interphases on micro and macro mechanical behavior of hexagonal-array fiber composites, *Transactions of ASME, Journal of Applied Mechanics*, 57 (1990) 956-963.

[6] R. M. Christensen, Mechanics of Composite Materials, Krieger Pub. Co., Florida, USA (1991).

[7] R. P. Nimmer, R. J. Bankert, E. S. Russel, G. A. Smith and P. K. Wright, Micromechanical modeling of fiber/matrix interface effects in transversely loaded SiC/Ti-6-4 metal matrix composites, *Journal of Composites Technology & Research*, 13 (1991) 3-13.

[8] D. B. Zahl and S. Schmauder, Transverse strength of continuous fiber metal matrix composites, *Computational Materials Science*, 3 (1994) 293-299.

[9] J. Lee and A. Mal, Characterization of matrix damage in metal matrix composites under transverse loads, *Computational Mechanics*, 21 (1998) 339-346.

[10] S. Naboulsi, Modeling transversely loaded metal-matrix composites, *Journal of Composite Materials*, 37 (2003) 55-72.

[11] M. M. Aghdam and S. R. Falahatgar, Micromechanical modeling of interface damage of metal matrix composites subjected to transverse loading, *Composite Structures*, 66 (2004) 415-420.

[12] J. K. Lee, H. D. Han and A. Mal, Effects of anisotropic fiber packing on stresses in composites, *Computer Methods in Applied Mechanics and Engineering*, 195 (33-36) (2006) 4544-4556.

[13] J. W. Ju and Y. F. Ko, Micromechanical elastoplastic damage modeling for progressive interfacial arc debonding for fiber reinforced composites, *International Journal of Damage Mechanics*, 17 (2008) 307-356.

[14] J. K. Lee, Elastic analysis of unbounded solids using volume integral equation method, *Journal of Mechanical Science and Technology*, 22 (3) (2008) 450-459.

[15] G. B. Jeffery, The motion of ellipsoidal particles immersed in a viscous fluid, *Proceedings of the Royal Society of London. Series A*, 102 (715) (1922) 161-179.

[16] S. K. Ghosh and H. Ramberg, Reorientation of inclusions by combination of pure shear and simple shear, *Tectonophysics*, 34 (1976) l-70.

[17] A. V. Cherkaev, Y. Grabovsky, A. B. Movchan and S. K. Serkov, The cavity of the optimal shape under the shear stresses, *International Journal of Solids and Structures*, 35 (33) (1998) 4391-4410.

[18] H. Shen, P. Schiavone, C. Q. Ru and A. Mioduchowski, Stress analysis of an elliptic inclusion with imperfect interface in plane elasticity, *Journal of Elasticity*, 62 (2001) 25-46.

[19] D. W. Schmid, Finite and Infinite Heterogeneities under Pure and Simple Shear, Ph.D. Dissertation, Geologisches Institut, ETH, Zürich, Switzerland (2002).

[20] D. W. Schmid and Y. Y. Podladchikov, Analytical solutions for deformable elliptical inclusions in general shear, *Geophysical Journal International*, 155 (2003) 269-288.

[21] S. H. Treagus and L. Lan, Simple shear of deformable square objects, *Journal of Structural Geology*, 25 (2003) 1993-2003.

[22] R. Shimomura and H. Hasegawa, In-plane shear of an infinite elastic plate containing a circular inclusion with a partially debonded interface, *The Computational Mechanics Conference, The Japan Society of Mechanical Engineers*, 17 (2004) 699-700.

[23] S. Vigdergauz, Shape optimization of a rigid inclusion in a shear-loaded elastic plane, *Journal of Mechanics of Materials and Structures*, 2 (2) (2007) 275-291.

[24] X. Wang, E. Pan and L. J. Sudak, Uniform stresses inside an elliptical inhomogeneity with an imperfect interface in plane elasticity, *Transactions of the ASME, Journal of Applied Mechanics*, 75 (2008) (054501-1)- (054501-5).

[25] A. K. Mal and L. Knopoff, Elastic wave velocities in two component systems, *Journal of the Institute of Mathematics and its Applications*, 3 (1967) 376-387.

[26] V. A. Buryachenko, Micromechanics of Heterogeneous Materials, Springer, New York, USA (2007).

[27] P. K. Banerjee, The Boundary Element Methods in Engineering, McGraw-Hill, England (1993).

[28] PATRAN User's Manual, Version 7.0, MSC/PATRAN (1998).

[29] A. K. Mal and S. J. Singh, Deformation of Elastic Solids, Prentice-Hall, New Jersey, USA (1991).

[30] ADINA User's Manual, Version 8.5, ADINA R & D, Inc. (2008).

[31] J. K. Lee, Volume integral equation method for multiple isotropic inclusion problems in an infinite solid under uniaxial tension, *Transactions of the Korean Society of Mechanical Engineers, A*, 34 (7) (2010) 881-889.

Jungki Lee is a professor at Hongik University (Jochiwon Campus). He received a Ph.D. in Mechanical Engineering from the University of California, Los Angeles, USA. His research interests are computational mechanics of solids, nondestructive evaluation, composite materials. He has developed the volume integral equation method (VIEM) with Professor Mal at UCLA.